

EFFECTIVE NONLINEAR ANALYSIS OF ARBITRARY THIN SHELLS BY SIMPLE
FINITE ELEMENTS

MICHAŁ KLEIBER
ANDRZEJ ZACHARSKI
IPPT PAN
Warszawa

1. Introduction

Available analytical solutions to structural problems of general shells are limited in scope and in general do not apply to arbitrary shapes, load conditions, irregular stiffening and support conditions, cut outs, and many other aspects of practical design. In the case of a simultaneous action of inelastic material properties and large deformations in free-form shells the situation is particularly difficult and successful analytical approaches even for simple geometries and loadings can hardly be expected. The finite element method has consequently come to the fore as an approach to structural analysis of shells because of its facility to deal with these complications. A comprehensive review of the history of the finite element developments for shell analysis can be found in [1]. This history evolved from very simple, flat elements to extremely complicated double curved elements and covered essentially the whole range of different approximations applied to the classical and nonclassical shell equations considered at the element level.

Unfortunately it is still fair to say that the final finite element formulation for nonlinear thin shell analysis is far from being settled. From the engineering point of view the prevailing problem is the lack of elements which can show both good accuracy and efficiency. The apparently better deeply curved elements quickly become so complicated that their attendant high computational cost have pretty well precluded the acceptance and general use of these elements. Their use seems to be particularly ruled out in the case of extensive nonlinearities of the problem which requires the element stiffnesses to be recalculated a large number of times. It is therefore understandable that the researches in the field of nonlinear shell analysis turned back to more simple elements. In this way, as concluded in [2], the history of the development of general shell finite elements has come full circle.

The simplest possible geometrical representation of a doubly curved shell surface is a facet approximation by flat elements. The extremely simple and efficient formulation that can be achieved by flat elements make them very well suited for nonlinear applications, in particular when used in the framework of the updated Lagrangian description of motion. The wide range of numerical examples studied in [3 - 11] indicate that flat finite elements may be very useful in the analysis of nonlinear shell problems. However, this approach has also its well-known deficiencies to mention only

- (a) the exclusion of the coupling of stretching and bending within the elements, (b) the difficulty of treating junctions where all elements are co-planar and (c) the presence of „discontinuity” bending moments, which do not appear in the continuously-curved actual structure, at the element juncture lines. Fortunately, many of these can be dealt with through various devices and additional computational effort.

The use of planar elements, in which the membrane and plate bending stiffness are derived from displacement patterns of different forms cannot insure complete compatibility of the assemblage which is needed for convergence of the sequence of finite element solutions to a true solution. (The second criterion necessary for convergence claims the following: the displacement functions have to be of such a form that if nodal generalized displacements are compatible with a constant strain condition such constant strain will in fact be obtained. Note that this criterion incorporates in fact the commonly quoted requirement of rigid body displacements as these are a particular case of constant strain displacement. In our approach the second criterion will always be satisfied).

The effect of the kinematic incompatibility can be expected to diminish with decreasing mesh size. In the present development an extensive study of this phenomenon has been made showing the essentially monotonic convergence to the true solution for a wide range of shell geometries and external loading patterns.

Formulating a nonlinear shell problem, one of the basic decisions implied by efficiency considerations is the selection of a frame of reference. For large displacement analysis of thin shells the total Lagrangian formulation has been adopted by most authors. As it is demonstrated in the following, however, the updated Lagrangian description offers remarkable simplifications in the formulation and this approach is used in this paper.

In the present study both the geometrical and material nonlinearities are taken into account. The former make it possible to solve the linearized and nonlinearized (solved by means of the step-by-step procedure) structural stability problems. The latter lead to the inelastic analysis performed basing upon an elasto-viscoplastic material model as proposed in [12] and subsequently discussed in [13 - 17]. This approach seems to have some significant advantages over the classical rate-independent elastic-plastic formulation. First it produces an additional numerical effect which stabilizes the iteration procedures used in the program. Second, it allows more rational generalizations towards the inclusion of the dynamic effects into the solution process. And third, it is in a certain sense more general approach as the classical elastoplastic solutions can be recovered in the limit as stationary non-viscous solutions of the viscous problem.

The presentation is necessarily brief and no explicit forms of the stiffness matrices are given. More details on both the theoretical and numerical parts of the study are available in [10, 11].

2. Coordinate systems

The geometry of the shell is replaced by an assembly of flat elements of triangular and/or quadrilateral shape (the latter elements being composed of four flat triangles not necessarily forming one plane), of Sec. 3. To describe the geometry and stiffness properties of the idealized structure we use the following coordinate systems, Fig. 1:

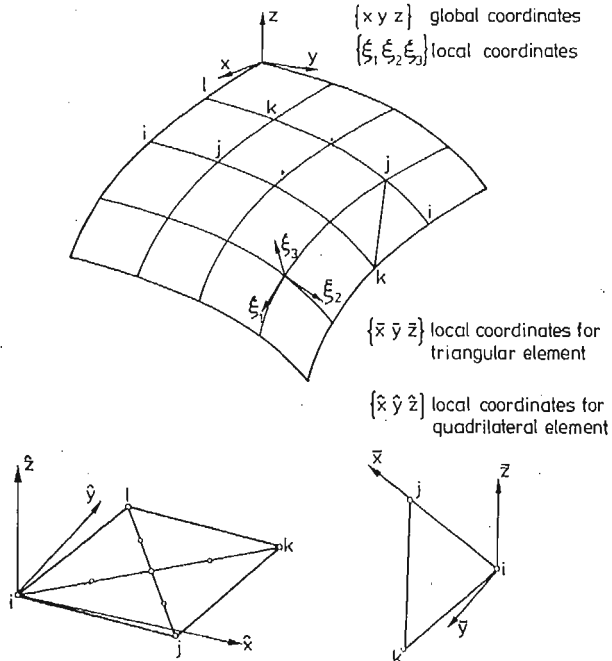


Fig. 1

- (a) global cartesian coordinate system $\{xyz\}$,
- (b) at each nodal point: moving (e.g. stepwise updated) surface coordinate system $\{\xi_1 \xi_2 \xi_3\}$ where ξ_3 — axis is always taken normal to the current shell surface while the ξ_1 — and ξ_2 — axes have the tangential directions at the particular nodal point,
- (c) for each triangular element: local cartesian coordinates $\{\bar{x}\bar{y}\bar{z}\}$,
- (d) for each triangular sub-element of a quadrilateral element: local cartesian coordinates $\{\bar{x}_\alpha \bar{y}_\alpha \bar{z}_\alpha\}$, $\alpha = 1, 2, 3, 4$,
- (e) for each quadrilateral element: local cartesian coordinates $\{\hat{x}\hat{y}\hat{z}\}$ with the axes \hat{x} and \hat{y} lying in an „averaged” plane „tangential” to the element. This plane is formed by minimizing the sum of the squares of the normal distances from the plane to the exterior nodes of the quadrilateral.

The common reference frame to which all element matrices are transformed prior to the assembly of stiffnesses is herein called base coordinates. There are two different possibilities to choose the base coordinates. We describe them briefly in Sec. 3.

3. Finite elements

The detailed description of the nonlinear formulation for shell elements used in the present analysis can be found in [11] and will be summarized below. Since shell behaviour is characterized by both membrane action and bending action it is essential to recognize

both of these in evaluating the element stiffness properties. Two finite elements are available in the program both being based on a flat triangular shell element as described in [10]:

- (a) plane triangular element with *eighteen* degrees of freedom¹⁾ composed of:
- (a1) linear displacement membrane element with six d.o.f. (three corner nodes with two in-plane displacement components at each of them),
 - (a2) fully compatible Kirchhoff plate element with twelve d.o.f. (one transverse displacement and two plate-type rotations at each of the corners and at the mid-point of the triangle). The element is in fact a super-element composed of three triangular elements allowing the C^1 — transverse displacement (full compatibility!) to vary as cubic polynomial within each triangular sub-element. In other words the transverse displacement approximation for the element is formed from the polynomial spline of the degree 3 and smoothness 1. We note also that the above properties imply the linear curvature variation within each sub-triangle.

Since the three mid-point plate-type d.o.f. are local to the element they are condensed (by means of the inverse Gauss elimination) prior to the assembly procedure. This results in the total number of **fifteen** d.o.f. for the triangular shell element (two membrane-type and three plate-type d.o.f. at each exterior, corner nodes),

- (b) non-plane quadrilateral element with forty one d.o.f. composed of four triangular elements each of them based upon,
- (b1) quadratic displacement membrane element with twelve d.o.f. (three corner and three mid-side nodes with two in-plane displacement components at each of them),
 - (b2) plate element described above, cf. (a2),

The external (with regard to the quadrilateral) boundaries of the four triangular elements are additionally constrained to deform linearly. These constraints eliminate the exterior mid-side nodes of the element, thereby reducing the connectivity (band width) which must be considered in the direct solution of the nodal point equilibrium equations. In this way the total number of d.o.f. is reduced to thirty three (forty one less two d.o.f. at each of the four mid-side nodes). Moreover, since there exist in the quadrilateral element thirteen d.o.f. which are local to the element, the corresponding static condensation reduces finally the global number of d.o.f. to **twenty**.

In this way we consistently end up with two finite element: triangular (three nodes) and quadrilateral (four nodes) with five d.o.f. at each node.

As we already mentioned in Sec. 2 the generalized displacements have to be transformed from local to a common frame of reference so that the assembly procedure could be effectively performed. It is here assumed that the rotational d.o.f. are always referred to the surface coordinates ξ_1 and ξ_2 . For the translational d.o.f. it is left to the user to choose between two common coordinate systems: the global system $\{xyz\}$ or the surface system $\{\xi_1 \xi_2 \xi_3\}$. In this way we can practically perform the assembly calculation either in a „mi-

¹⁾ The term „degrees of freedom” will be further referred to as d.o.f.

ned" coordinate system (the rotational d.o.f. in the $\{\xi_1 \xi_2 \xi_3\}$ coordinates, the translational d.o.f. in the $\{x, y, z\}$ coordinates) or in the surface coordinate system alone (all the d.o.f. referred to the $\{\xi_1 \xi_2 \xi_3\}$ coordinates).

4. Incremental description of motion and the solution procedure

It is generally accepted that the incremental approach is the most effective way of handling nonlinear structural problems. In the case of elastic structures it is only an alternative to other solution algorithms while for the inelastic structures the step-by-step approach is in general unavoidable because of the incremental nature of the material response. The solution algorithm accepted in the present paper relies entirely on the stepwise linearized solutions which enable us to trace the characteristic load — displacement curves describing the nonlinear behaviour of the shell structures analysed. At each solution step an iteration algorithm over the residual out-of-balance forces is planned to be additionally implemented to improve the solution by restoring exact equilibrium. The solution algorithm is controlled by parameters that are input to the computer program.

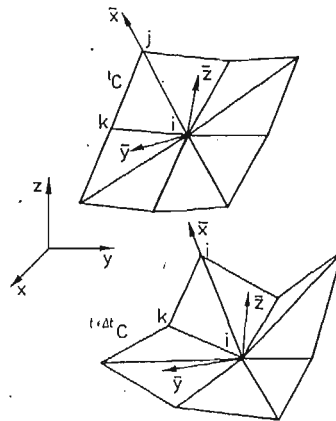


Fig. 2

A typical triangular element with the nodes 1 - 2 - 3 will be referred to the local cartesian coordinates $\{\bar{x} \bar{y} \bar{z}\}$, Fig. 2. The \bar{x} -axis is taken to coincide with the middle line of the 1 - 2 side of the triangle, the \bar{y} -axis lies in the element middle plane and is directed towards the node 3 while the \bar{z} -axis is chosen so that the $\{\bar{x} \bar{y} \bar{z}\}$ — system be right-handed. The unit vectors of the system are built a new at each incremental step basing upon new nodal coordinates and in accordance with the above definition.

We assume that the solution for the kinematic and static variables for all time steps from a time t_0 to the current time t , inclusive, is known, and that the solution for time $t + \Delta t$ is required next. According to the concept of the updated Lagrangian description we take the configuration ${}^t C$ at time t as a reference state to describe the incremental motion ${}^t C \xrightarrow{t+\Delta t} C$, Fig. 3. Referring to this configuration we introduce in the plane of the element the second Piola-Kirchhoff stress tensor $S_{A\Delta} \Delta$, $A = 1, 2$ which describes

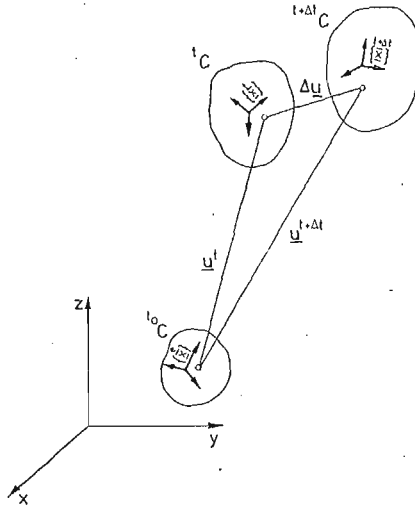


Fig. 3

the current stress at time t , and the Green strain tensor E_{AA} , $A, A = 1, 2$ which describe the current strain in the element. The stresses S_{AA} are assumed to be equilibrated by the given external forces p_k $k = 1, 2, 3$ acting upon the shell.

The incremental changes of the load are denoted by Δp_k ; they give rise to incremental stresses ΔS_{AA} , incremental strains ΔE_{AA} and incremental displacements ΔU_A , ΔW , the latter referred to the \bar{x} , \bar{y} , \bar{z} directions, respectively. The new total stresses $S_{AA} + \Delta S_{AA}$ are assumed to be in the equilibrium with the new total external forces $p_k + \Delta p_k$.

The incremental strain displacement relationship is taken in the form

$$\Delta E_{AA} = \frac{1}{2} (\Delta u_{A,A} + \Delta u_{A,A}) + \frac{1}{2} \Delta W_{,A} \Delta W_{,A} - \bar{Z} \Delta W_{,AA}, \quad (1)$$

which means that the only geometric nonlinear effect included in the formulation is the influence of the transverse displacement upon the membrane strains. It is broadly known that the results obtained within this approximation are sufficiently accurate for majority of mildly nonlinear practical problems.

We introduce next the shape functions for the triangular plate element as

$$\Delta u_{A2 \times 1} = \hat{\Phi}_{A2 \times 15}^T \Delta u_{15 \times 1}^{(N)}, \quad (2)$$

$$\Delta W_{1 \times 1} = \hat{\Phi}_{1 \times 15}^T \Delta u_{15 \times 1}^{(N)}, \quad (3)$$

where the vector $\Delta U^{(N)}$ collects the generalized nodal displacements for the element considered. Its conjugate internal nodal force vector $U_{15 \times 1}^{(N)}$ satisfies the virtual work equation of the form

$$\int_V S_{AA} \delta E_{AA} dV = U_{1 \times 15}^{(N)T} \delta u_{15 \times 1}^{(N)}, \quad (4)$$

where V is the element volume, $\delta \mathbf{u}^{(N)}$ is an arbitrary (virtual) variation of the displacement vector and δE_{AA} is the corresponding variation of E_{AA} taken for $\Delta u_A = \Delta W = 0$, e.g. at the beginning of the step considered (in the configuration $'C$)

$$\delta E_{AA} = \frac{1}{2} (\delta u_{A,A} + \delta u_{A,A}) - \bar{z} \delta w_{,AA}. \quad (5)$$

For the configuration ${}^{t+\Delta t}C$ we write the similar virtual work equation as

$$\int_V (S_{AA} + \Delta S_{AA}) \delta E_{AA} dV = (\mathbf{U}^{(N)} + \Delta \mathbf{U}^{(N)})_{1 \times 15}^T \delta \mathbf{u}_{15 \times 1}^{(N)}, \quad (6)$$

where now δE_{AA} is the variation of E_{AA} taken in the new configuration ${}^{t+\Delta t}C$, e.g.

$$\delta E_{AA} = \frac{1}{2} (\delta u_{A,A} + \delta u_{A,A}) + \frac{1}{2} (\delta w_{,A} w_{,A} + w_{,A} \delta w_{,A}) - \bar{z} \delta w_{,AA}. \quad (7)$$

By using eqs. (4) - (7) we immediately get

$$\begin{aligned} \Delta \mathbf{U}^{(N)T} \delta \mathbf{u}^{(N)} = & \int_V \left\{ S_{AA} \frac{1}{2} (\delta w_{,A} w_{,A} + w_{,A} \delta w_{,A}) + \right. \\ & \left. + \Delta S_{AA} \left[\frac{1}{2} (\delta u_{A,A} + \delta u_{A,A}) + \frac{1}{2} (\delta w_{,A} w_{,A} + w_{,A} \delta w_{,A}) - \bar{z} \delta w_{,AA} \right] \right\} dV \end{aligned} \quad (8)$$

Noting the symmetry of S_{AA} and ΔS_{AA} and neglecting the third-order terms eq. (8) can be conveniently written as

$$\Delta \mathbf{U}^{(N)T} \delta \mathbf{u}^{(N)} = (\Delta \bar{\mathbf{U}}_{\beta}^{(N)} + \Delta \bar{\bar{\mathbf{U}}}_{\beta}^{(N)}) \delta u_{\beta}^{(N)}, \quad (9)$$

where β runs over the sequence 1, 2, ..., 15; the summations with respect to β is implicitly assumed on the right-hand side of eq. (9),

$$\Delta \bar{\bar{\mathbf{U}}}_{\beta}^{(N)} = \left(\int_V S_{AA} \hat{\Phi}_{,A}^{\beta} \hat{\Phi}_{,A}^{\alpha} dV \right) \Delta u_{\alpha}^{(N)}, \quad (10)$$

in the nonlinear contribution to the nodal incremental forces while

$$\Delta \bar{\mathbf{U}}^{(N)} = \int_V \Delta S_{AA} \left[\frac{1}{2} (\hat{\Phi}_{A,A}^{\beta} + \hat{\Phi}_{A,A}^{\beta}) - \bar{z} \hat{\Phi}_{,AA}^{\beta} \right] dV, \quad (11)$$

describes the corresponding linear contribution. Defining the resultant forces by

$$N_x = \int_{-h/2}^{h/2} S_{xx} dz, \quad N_y = \int_{-h/2}^{h/2} S_{yy} dz, \quad N_{xy} = \int_{-h/2}^{h/2} S_{xy} dz, \quad (12)$$

and the resultant moments by

$$M_x = \int_{-h/2}^{h/2} S_{xx} \bar{z} dz, \quad M_y = \int_{-h/2}^{h/2} S_{yy} \bar{z} dz, \quad M_{xy} = \int_{-h/2}^{h/2} S_{xy} \bar{z} dz \quad (13)$$

eqs. (10), (11) can be transformed to the form

$$\Delta \bar{\bar{\mathbf{U}}}_{15 \times 1}^{(N)} = \left(\int_A (\nabla \hat{\Phi})_{15 \times 2} N_{2 \times 2} (\nabla \hat{\Phi})_{2 \times 15}^T dA \right) \Delta \mathbf{u}_{15 \times 1}^{(N)}, \quad (14)$$

$$\Delta \bar{\mathbf{U}}_{15 \times 1}^{(N)} = \int_A (\mathbf{B}_{m15 \times 3} \Delta \mathbf{N}_{3 \times 1} - \mathbf{B}_{b15 \times 3} \Delta \mathbf{M}_{3 \times 1}) dA \quad (15)$$

where A is the triangle area and

$$N_{2 \times 2} = \begin{bmatrix} N_{xx} & N_{xy} \\ N_{xy} & N_{yy} \end{bmatrix}, \quad (16)$$

$$\Delta N_{3 \times 1} = \{\Delta N_{xx} \Delta N_{yy} \Delta N_{xy}\}, \quad (17)$$

$$\Delta M_{3 \times 1} = \{\Delta M_{xx} \Delta M_{yy} \Delta M_{xy}\}, \quad (18)$$

$$\nabla \hat{\Phi}_{15 \times 2} = \begin{bmatrix} \Phi_{,x}^1 & \Phi_{,y}^1 \\ \Phi_{,x}^2 & \Phi_{,y}^2 \\ \vdots & \vdots \\ \Phi_{,x}^{15} & \Phi_{,y}^{15} \end{bmatrix}, \quad (19)$$

$$Bm_{15 \times 3} = \begin{bmatrix} \Phi_{x,x}^1 & \Phi_{y,y}^1 & \Phi_{y,x}^1 + \Phi_{x,y}^1 \\ \vdots & \vdots & \vdots \\ \Phi_{x,x}^{15} & \Phi_{y,y}^{15} & \Phi_{y,x}^{15} + \Phi_{x,y}^{15} \end{bmatrix}, \quad (20)$$

$$B_{b15 \times 3} = \begin{bmatrix} \hat{\Phi}_{,xx}^1 & \hat{\Phi}_{,yy}^1 & 2\hat{\Phi}_{,xy}^1 \\ \hat{\Phi}_{,xx}^{15} & \hat{\Phi}_{,yy}^{15} & 2\hat{\Phi}_{,xy}^{15} \end{bmatrix}. \quad (21)$$

The incremental forces and moments in eq. (15) are defined by replacing in the definitions (12), (13) the stress components S_{AA} by the corresponding incremental stress components ΔS_{AA} .

Due to the arbitrariness of the variations $\delta u^{(N)}$ eq. (9) yields the increment of the internal nodal generalized force vector as

$$\Delta U^{(N)} = \Delta \bar{U}^{(N)} + \Delta \bar{\bar{U}}^{(N)}. \quad (22)$$

In order to maintain the equilibrium at a given node of the discretization mesh the sum $\Delta R^{(int)}$ of the internal generalized incremental forces coming from all the neighbouring elements must be equal to the external load $\Delta R^{(ext)}$ acting upon this node, e.g.

$$\Delta R^{(int)} = \Delta R^{(ext)}, \quad (23)$$

where this equality is meant to represent the incremental equilibrium of all the nodes of the discretized shell. Expressing the vector $\Delta R^{(int)}$ in terms of the components of the elemental vector $\Delta U^{(N)}$ in which in turn we use the relationships (14), (15) and appropriate incremental constitutive law, we end up with the relation of the form

$$\Delta R^{(int)}(\Delta r) = \Delta R^{(ext)} \quad (24)$$

where Δr is the vector of the generalized displacements of the whole assemblage of the shell finite elements. The explicit form of eq. (24) is regarded as the fundamental relationship for the static incremental analysis of shells. Such an explicit evaluation of all the matrices used above is disregarded here; the reader is referred to [10, 11] for the details.

The elemental geometric stiffness matrix is defined as

$$k_{15 \times 15}^{(g)} = \int_A \nabla \hat{\Phi} N (\nabla \hat{\Phi})^T dA \quad (25)$$

The geometric stiffness matrix was implemental in the program in a slightly modified version. This so-called inconsistent formulation corresponds to the fact that the shape

functions $\hat{\Phi}$ used in the derivation of $\mathbf{k}^{(o)}$ was different (simpler) than that used to obtain the constitutive stiffness matrix to be discussed below. As stated in [18], for instance, such an approximation leads to practically acceptable results allowing the significant computer time savings as compared to the consistent geometric stiffness evaluation.

We note that in order to calculate the force vector $\Delta\bar{\bar{U}}^{(N)}$ (or the geometric stiffness matrix $\mathbf{k}^{(o)}$) the state of stress at the beginning of step is the essential information required. In contrast, the evaluation of the vector $\Delta\bar{U}^{(N)}$ requires the material properties of the element to be known.

Let us start with the assumption of the linear elastic behaviour of the shell material, e.g.

$$\begin{bmatrix} \Delta S_{xx} \\ \Delta S_{yy} \\ \Delta S_{xy} \end{bmatrix} = \frac{\mathbf{E}}{1-\nu^2} \begin{bmatrix} 1 & \nu & 0 \\ \nu & 1 & 0 \\ 0 & 0 & \frac{1-\nu}{2} \end{bmatrix} \begin{bmatrix} \Delta E_{xx} \\ \Delta E_{yy} \\ \Delta E_{xy} \end{bmatrix} \quad (26)$$

which more compactly reads

$$\Delta S_{3 \times 1} = \mathbf{D}_{3 \times 3} \Delta \mathbf{E}_{3 \times 1} \quad (27)$$

where \mathbf{E} is the Young modulus and ν the Poisson ratio.

We write next eq. (1) as

$$\Delta \mathbf{E}_{3 \times 1} = \Delta \bar{\mathbf{E}}_{3 \times 1} + \Delta \bar{\bar{\mathbf{E}}}_{3 \times 1}, \quad (28)$$

where $\Delta \bar{\mathbf{E}}$ and $\Delta \bar{\bar{\mathbf{E}}}$ are the corresponding linear and nonlinear (with respect to the incremental displacements) parts of the incremental strain.

The vector $\Delta \bar{\mathbf{E}}$ is defined as

$$\Delta \mathbf{E}_{3 \times 1} = [\mathbf{B}_{m3 \times 15}^T - \bar{z} \mathbf{B}_{b3 \times 15}^T] \Delta \mathbf{u}_{15 \times 1}^{(N)} \quad (29)$$

with the matrices \mathbf{B}_m , \mathbf{B}_b given in eqs. (20), (21). Without recalling explicitly the definition of the nonlinear part we note only that the appropriate expression is independent of the coordinate \bar{z} , cf. eq. (1). By using eqs. (26) - (29) we arrive at

$$\Delta S = \mathbf{D} \Delta \mathbf{E} = \mathbf{D} [(\mathbf{B}_m^T - \bar{z} \mathbf{B}_b^T) \Delta \mathbf{u}^{(N)} + \Delta \bar{\bar{\mathbf{E}}}] \quad (30)$$

or, performing the linearization, at

$$\Delta S = \mathbf{D} [(\mathbf{B}_m^T - \bar{z} \mathbf{B}_b^T) \Delta \mathbf{u}^{(N)}]. \quad (31)$$

The generalization of the above approach to include the inelastic analysis capability is achieved here by specifying an inelastic constitutive law to be used instead of the elastic law given by eq. (26). The analysis will be based upon the elasto-viscoplastic constitutive assumptions first proposed in [12] and later explored numerically by many authors, [13 - 17].

The elastic-viscoplastic material is defined by the following constitutive relation

$$\Delta S = \mathbf{D} (\Delta \mathbf{E} - \Delta \mathbf{E}^{(vp)}) \quad (32)$$

where the only new quantity (as compared to eq. (26)) is the viscoplastic strain increment $\Delta \mathbf{E}^{(vp)}$ derived from

$$\Delta \mathbf{E}^{(vp)} = \gamma \Delta t \langle \Phi(F) \rangle \frac{\partial f}{\partial S}. \quad (33)$$

Here, γ is a material viscosity coefficient which has dimension (time)⁻¹, Δt is the time increment, $f(S)$ is a yield function entering the yield condition as

$$f(S) \leq \bar{\sigma}_0^2, \quad (34)$$

where $\bar{\sigma}_0$ is a current yield point stress determined in the uniaxial tension test,

$$F(S) = \frac{f(S) - \bar{\sigma}_0^2}{\bar{\sigma}_0^2} \quad (35)$$

and $\langle \Phi(F) \rangle$ is a discontinuous function of F which ensures that no viscoplastic flow occurs below the yield condition, e.g.

$$\langle \Phi(F) \rangle = \begin{cases} \Phi(F) & \text{if } F \geq 0, \\ 0 & \text{if } F < 0. \end{cases} \quad (36)$$

According to the above assumptions inelastic deformations will develop only when a threshold value for the state of stress corresponding to a yield surface is exceeded, and the viscoplastic strain increment is the function of the amount by which the stress exceeds this yield surface. The viscoplastic strain increment depends also on the material viscosity. In other words, the viscoplastic flow commences when the stress path penetrates the static yield condition and continues until stresses relax back to the current loading surface.

We assume further for simplicity

$$\Phi(F) = F, \quad (37)$$

For the Huber-Mises yield condition under the plane stress condition we have

$$f(S) = \frac{1}{2} [(S_{xx} - S_{yy})^2 + S_{xx}^2 + S_{yy}^2 + 6S_{xy}^2], \quad (38)$$

which, by (33), (35) leads to

$$\Delta \mathbf{E}_{3 \times 1}^{(vp)} = \gamma \Delta t \left(\frac{\frac{1}{2} [(S_{xx} - S_{yy})^2 + S_{xx}^2 + S_{yy}^2 + 6S_{xy}^2] - \bar{\sigma}_0^2}{\bar{\sigma}_0^2 \sqrt{5S_{xx}^2 + 5S_{yy}^2 - 3S_{xx}S_{yy} + 36S_{xy}^2}} \right) \begin{bmatrix} 2S_{xx} - S_{yy} \\ 2S_{yy} - S_{xx} \\ 6S_{xy} \end{bmatrix}. \quad (39)$$

The square root in the denominator on the right-hand side of (39) is introduced to normalize the vector $\frac{\partial f}{\partial S}$.

For hardening materials the yield limit $\bar{\sigma}_0$ changes in the course of the deformation process. We postulate the hardening law as a function of the total viscoplastic strains in the general form

$$\bar{\sigma}_0 = \bar{\sigma}_0(\mathbf{E}^{(vp)}). \quad (40)$$

Which has to be specified for a given material. We note that in inviscid plasticity calculations the explicit relation of the above type is not used directly²⁾ — the actual value of the yield stress $\bar{\sigma}_0$ is determined from the actual stress state by using the yield condition (34). In viscoplasticity, however, the yield condition is not a real constraint imposed on the constitutive relation as in general

$$f(S) - \bar{\sigma}_0 \neq 0. \quad (41)$$

²⁾ Eq. (40) enters the constitutive relation, though.

Denoting the intensities of the incremental stresses and inelastic strains by

$$\Delta S_i = \sqrt{(\Delta S_{xx})^2 + (\Delta S_{yy})^2 - \Delta S_{xx} \Delta S_{yy} + 3(\Delta S_{xy})^2}, \quad (42)$$

$$\Delta E_{(i)}^{(op)} = \frac{2}{3} \sqrt{3[(\Delta E_{xx}^{(op)})^2 + (\Delta E_{yy}^{(op)})^2 + \Delta E_{xx}^{(op)} \Delta E_{yy}^{(op)} + (\Delta E_{xy}^{(op)})^2]}. \quad (43)$$

(the latter definition takes into account the inelastic incompressibility of the material), and assuming that $\bar{\sigma}_0 = \bar{\sigma}_0(E_{(i)})$, we define the hardening modulus as

$$h = \frac{\Delta S_{(i)}}{\Delta E_{(i)}^{(op)}}. \quad (44)$$

Using eqs. (31) and (32) we arrive at

$$\Delta S = D[B_m^I - \bar{z}B_b^T] \Delta u^{(N)} - \Delta E^{(op)}. \quad (45)$$

Performing the integrations (12), (13), for the value of ΔS given by eq. (45) we get incremental membrane forces

$$\Delta N_{3 \times 1} = h \bar{D}_{3 \times 3} B_{m,15}^T \Delta U_{15 \times 1}^{(N)} - \Delta N^* \quad (46)$$

and the incremental bending moments

$$\Delta M_{3 \times 1} = -\frac{h^3}{12} \bar{D}_{3 \times 3} B_{b,15}^T \Delta u_{15 \times 1}^{(N)} - \Delta M^*, \quad (47)$$

where the „initial” generalized forces ΔN^* and ΔM^* are defined by

$$\Delta N^* = D \int_{-h/2}^{h/2} \Delta E^{(op)} dz, \quad (48)$$

$$\Delta M^* = D \int_{-h/2}^{h/2} \Delta E^{(op)} \bar{z} dz. \quad (49)$$

Similarly as before, cf. eq. (15) the expression for $\Delta \bar{U}_{15 \times 1}^{(N)}$ can now be obtained in the form

$$\begin{aligned} \Delta U_{15 \times 1}^{(N)} &= \int_A \left[B_m (h \bar{D} B_m^I \Delta u^{(N)} - \Delta N^*) + B_b \left(-\frac{h^3}{12} \bar{D} B_b^T \Delta u^{(N)} - \Delta M^* \right) \right] dA = \\ &= k^{(e)} \Delta u^{(N)} - \Delta U^{(N)*} \end{aligned} \quad (50)$$

where $k^{(e)}$ is the elastic elemental stiffness matrix used in the linear version of the program, [10] and based now on the current configuration at the beginning of the load step, and $\Delta U^{(N)*}$ forms a vector of the „additional” incremental nodal forces and moments defined by

$$\Delta U^{(N)*} = \int_A [B_m \Delta N^* - B_b \Delta M^*] dA. \quad (51)$$

The last two expressions suggest an iterative „initial force” procedure to be performed at each incremental step.

The application of the direct assembly procedure leads to the fundamental matrix equation describing the large displacement inelastic shell problem in the form

$$[K^{(e)} + K^{(e)}] \Delta r = \Delta R^{(ex)} + \Delta R^* \quad (52)$$

in which the matrices $\mathbf{K}^{(e)}$, $\mathbf{K}^{(o)}$ and the vectors Δr , $\Delta \mathbf{R}^*$ are the global counterparts of the elemental matrices $k^{(e)}$, $k^{(o)}$ and the vector $\Delta \mathbf{u}^{(N)}$, $\Delta \mathbf{U}^{(N)*}$ while $\Delta \mathbf{R}^{(\text{ext})}$ is the external load vector, cf. eq. (23). Because in the case of inelastic material properties there is no linear stress distribution across the thickness of the shell (and, in fact, no functional approximation for such a stress distribution can be rationally assumed a priori), the shell element is considered as composed of layers. To effectively find the inelastic elemental nodal forces we proceed as follows:

1. From eq. (39) the incremental inelastic strain is calculated for the given stress \mathbf{S} in all layers at each nodal point.
2. Using the trapezoidal rule the across-thickness integrations are performed according to eqs. (48), (49) resulting in the initial membrane forces $\Delta \mathbf{N}^*$ and bending moments $\Delta \mathbf{M}^*$.
3. Eq. (41) is used to find the initial nodal generalized forces $\Delta \mathbf{U}^{(N)*}$. Numerical area integration is carried out at this stage by simply assuming

$$\Delta \mathbf{U}^{(N)*} = \frac{1}{3} A \sum_{i=1}^3 (\mathbf{B}_{m_i} \Delta \mathbf{N}_i^* - \mathbf{B}_{b_i} \Delta \mathbf{M}_i^*) \quad (53)$$

where the index „ i ”, $i = 1, 2, 3$, refers to the nodal values of the triangular element.

4. Eq. (52) is obtained as a result of the direct assembly procedure. It is then solved for $\Delta \mathbf{r}$, and this calculation is followed by:

- evaluation of the new incremental stresses by eq. (45),
- evaluation of the new total stresses according to the known stress accumulation procedure,
- evaluation of the new „initial load” vector
- solution of eq. (52) for the improved value of the incremental displacement $\Delta \mathbf{r}$.

The iteration process is continued until convergence is achieved up to a desired accuracy. In the present study the convergence is monitored by using alternatively the conditions:

$$\frac{\|\Delta \mathbf{R}^{(k)*} - \Delta \mathbf{R}^{*(k-1)}\|}{\|\Delta \mathbf{R}^{*(k-1)}\|} < \text{tol}(R)$$

$$\frac{\|\Delta \mathbf{r}^{(k)} - \Delta \mathbf{r}^{(k-1)}\|}{\|\Delta \mathbf{r}^{(k-1)}\|} < \text{tol}(r)$$

where k stands for the k -th iteration.

5. Linearized stability analysis

For one-parameter (proportional) loadings the fundamental matrix equation describing the static problem of elastic thin shells can be presented in a convenient, approximate form as, cf. eq. (52)

$$[\mathbf{K}^{(e)} + \lambda \mathbf{K}^{(o)}(\sigma_*)] \Delta \mathbf{r} = \lambda \mathbf{R}_*^{(\text{ext})} \quad (54)$$

where $K^{(o)}(\sigma^*)$ signifies symbolically dependence of the initial stress matrix on the stress state σ^* which corresponds linearly to a reference external load $R_{*}^{(ex)}$ while λ is the scalar load multiplier. The approximation in eq. (54) consists essentially in using the initial coordinates for setting up the stiffness matrices $K^{(e)}$ and $K^{(o)}$, which is rigorously valid for small deformation problems only.

The purpose of the linearized analysis of the shell stability is to check the uniqueness of the solution Δr of eq. (54) for each given value of the parameter λ . The points of such a non-uniqueness are called bifurcation (or branching) points on the primary equilibrium path in the load-displacement space $\lambda - \Delta r$. According to the definition at the bifurcation point $\lambda = \lambda_{cr}$ the relations hold

$$\begin{aligned} [K^{(e)} + \lambda_{cr} K^{(o)}(\sigma^*)] \Delta r_1 &= \lambda_{cr} R_{*}^{(ex)}, \\ [K^{(e)} + \lambda_{cr} K^{(o)}(\sigma)] \Delta r_2 &= \lambda_{cr} R_{*}^{(ex)} \end{aligned} \quad (55)$$

which, when subtracted from each other, yield

$$[K^{(e)} + \lambda_{cr} K^{(o)}(\sigma)] v = 0, \quad (56)$$

with

$$v = \Delta r_1 - \Delta r_2. \quad (57)$$

Eq. (56) represents a generalized eigenvalue problem which yields as its solution the N different critical load parameters³⁾ $\lambda_{cr}^1, \lambda_{cr}^2, \dots$ and the corresponding buckling modes v_1, v_2, \dots . In most practical situations only the first pair (λ_{cr}^1, v_1) is important which greatly simplifies the computations.

In the present program the eigenvalue problem (56) is solved by using the so-called subspace iteration method.

6. Computer studies

- I. Linear analysis of a rectangular plate with complex boundary conditions, Fig. 4. The plate is subjected to uniformly distributed pressure load. Two finite element idealizations are shown in Fig. 4. In Tabl. 1. The present numerical results are compared against the analytical results reported in [19].
- II. Linear analysis of a clamped, axisymmetric sphere under the point load applied at the apex, Fig. 5. The part of the shell considered in the analysis and its finite element idealization are shown in Fig. 5. The results are discussed in Tabl. 2.
- III. Geometrically nonlinear analysis of a quadratic plate clamped at the boundaries, Fig. 6. The plate is subjected to uniformly distributed pressure load. The loading was assumed to act perpendicularly deforming surface of the plate. Fig. 6 and 7 illustrate the computed variation of the vertical displacement at the center point of the plate

³⁾ The so-called multiple bifurcation points are excluded here to simplicity is the total number of degrees of freedom in the discretized shell.

v_s , the applied load and the computed variations of the normal stresses on both the upper and lower surfaces at the center point v_s , the applied load, respectively. The agreement of the results with those discussed in [20] is excellent.

IV. Geometrically nonlinear analysis of a circular cylindrical shell, Fig. 8.

The shell is subjected to a point load applied centrally on the convex side. The longitudinal boundaries are hinged and immovable, whereas the curved edges are

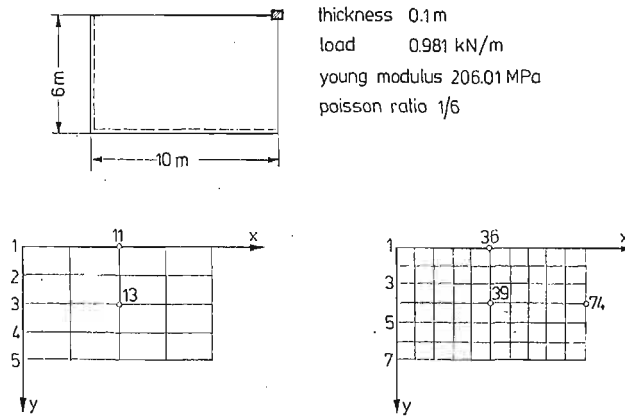


Fig. 4

Table 1

		w [m]	M_2 [kN]	M_1 [kN]
$x = \frac{a}{2}, y = \frac{a}{2}$ Node 13 (16 el) Node 39 (60 el)	N 16	0.002477	3.777	3.063
	N 60	0.002688	3.947	3.136
	A	0.002667	3.600	2.649
$x = \frac{a}{2}, y = 0$ Node 11 (16 el) Node 36 (60 el)	N 16	0.003972	6.511	
	N 60	0.004356	6.875	
	A	0.004330	7.250	
$x = a, y = \frac{b}{2}$ Node 23 (16 el) Node 74 (60 el)	N 16	0.001070		4.707
	N 60	0.001121		5.049
	A	0.001222		5.366

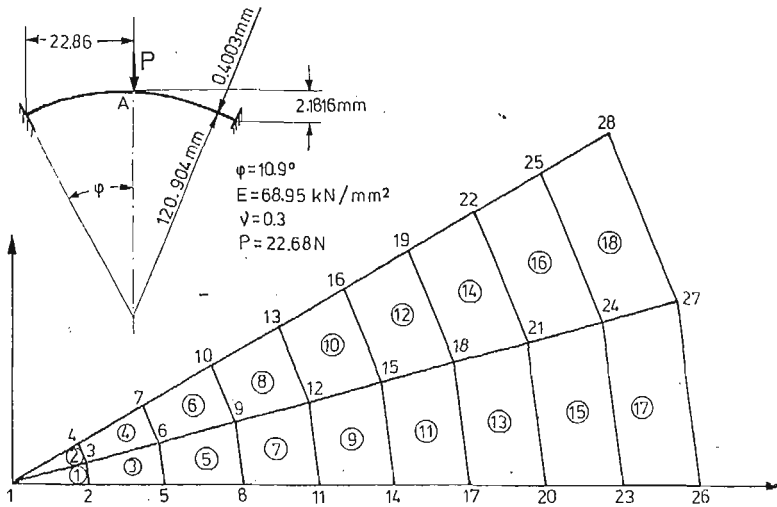


Fig. 5

Table 2

	w_A [mm]	M_A [N]
analytical solution	0.090932	-8.2312
finite difference method	0.093472	
present solution	0.091440	-7.7058
error %	0.56	6.38

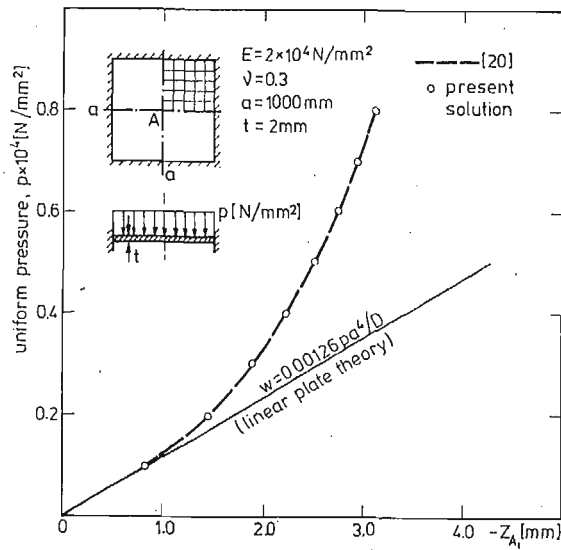


Fig. 6

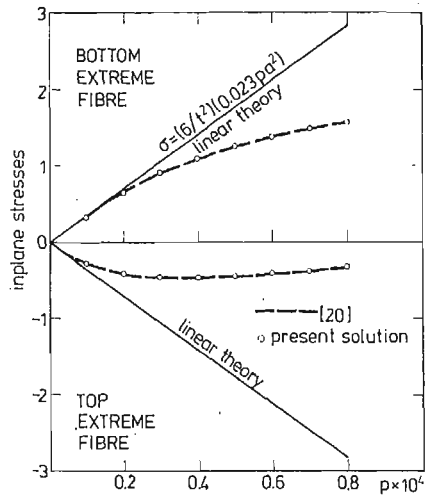


Fig. 7

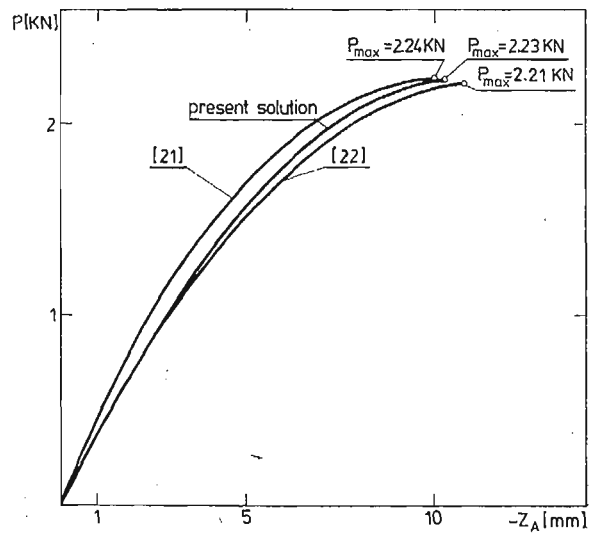
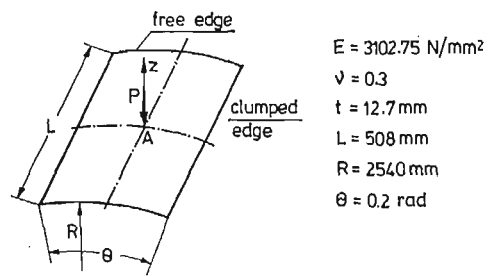


Fig. 8

completely free. The analysis was continued up to the point at which singularity of the total stiffness matrix appeared. One-quarter of the panel was discretized by a 6×6 finite element mesh. The comparison of the present results with those discussed in [21], [22] is shown in Fig. 8. Good agreement of the results is observed.

V. Geometrically nonlinear analysis of another cylindrical shell, Fig. 9.

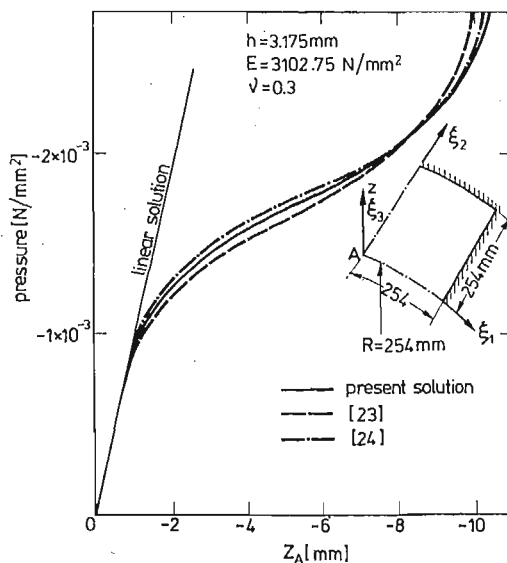


Fig. 9

The circular cylindrical shell portrayed in Fig. 9, is clamped along all four boundaries and subjected to uniform inward radial loading. One-quarter of the shell was discretized by an uniform 8×8 finite element mesh and 32 equal load steps were applied. Fig. 9 shows a very good agreement of the present results as compared against those given in [23], [24]. Almost the same results were obtained in the present study by using an uniform 6×6 mesh and 40 load increments.

VI. Geometrically nonlinear analysis of a spherical shell, Fig. 10.

The shell is subjected to a concentrated load at the apex; all edges are hinged and immovable. One-quarter of the shell was discretized by a 6×6 finite element mesh and 40 load increments were used. As a matter of fact the problem was considered under the apex displacement control rather than under the force control. This made it possible to get through the limit point on the load-displacement diagram without any difficulties. The results were found to be sufficiently accurate, cf. Fig. 10 cf. [23], their further improvement is possible by simply using more load increments.

VII. Limit load analysis of a quadratic plate, under uniform loading, Fig. 11.

The upper and lower limit load estimates are given as, cf. [25]

$$p_s = \frac{24M_0}{a^2}, \quad M_0 = \frac{1}{2} \bar{\sigma}_0 h^2.$$

$$p_k = \frac{2}{\sqrt{3}} p_s$$

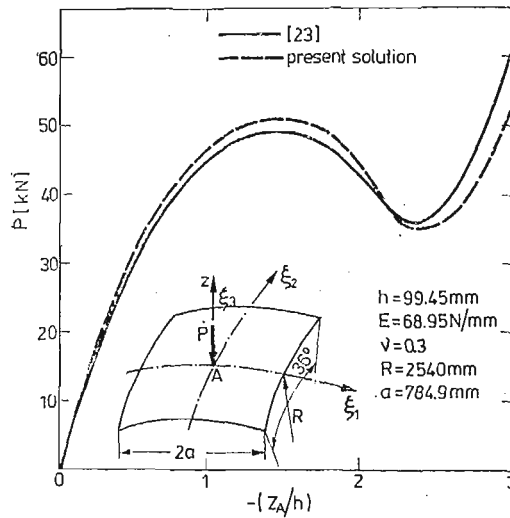


Fig. 10

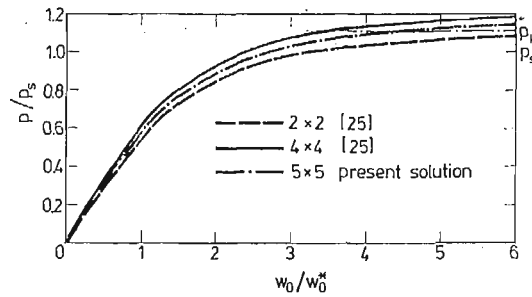
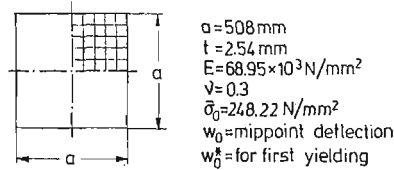
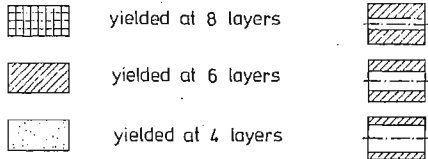
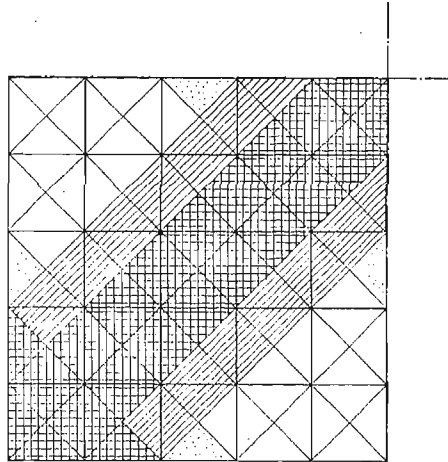


Fig. 11

The 5×5 finite element mesh was used each element consisting of 11 layers assumed for the observation of the across-thickness plastic zone development. The results of the analysis are shown in Fig. 11, 12.

VIII. Inelastic, large displacement analysis of a spherical cap, Fig. 13.

The shell is hinged at the boundary and subjected to a concentrated force acting at the apex. The material and geometric data are the same as in Example II, cf. Fig. 5. The material is assumed to be ideally plastic with $\bar{\sigma}_0 = 137.9 \text{ N/mm}^2$. The displacement control of the process was used. The first five incremental apex displacements were assumed to be equal to -0.0254 mm , which was followed by the



$$P/P_s = 1$$

Fig. 12

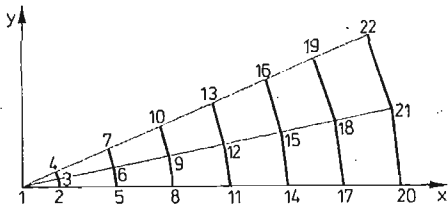


Fig. 13

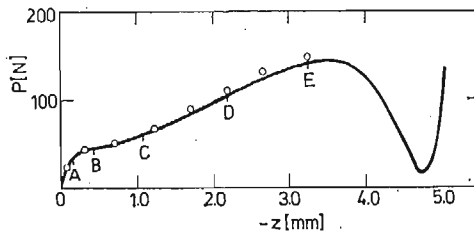


Fig. 14

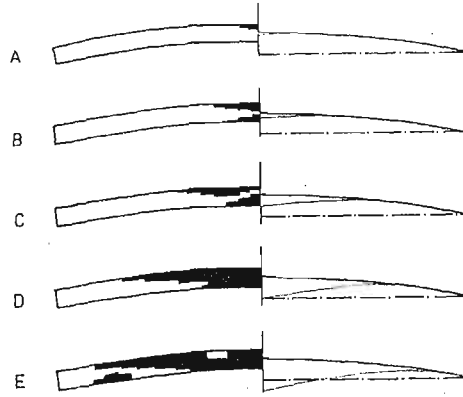


Fig. 15

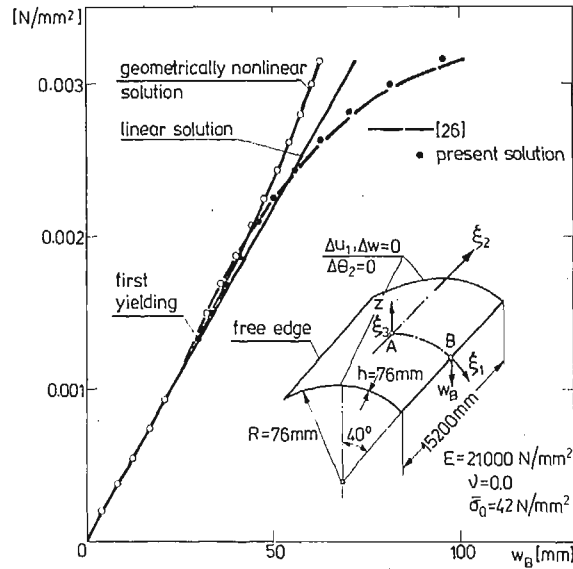


Fig. 16

25 steps of -0.127 mm. The present results are shown in Fig. 14 and 15 and compared with those given in [7].

IX. Inelastic, large displacement analysis of a cylindrical panel, Fig. 16.

The shell is subjected to the uniformly distributed loading acting in the negative z -direction.

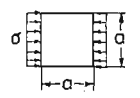
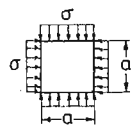
The load was assumed to increase from 0 to 0.00315 N/mm² in the 24 equal increments. The results are given in Fig. 16 cf. [26].

X. Linearized stability of elastic quadratic plates, Tabl. 3.

The linearized stability formulation described in Sec. 5 was the base for calculating the buckling loads for the two differently supported plates. One-quarter of the

plate was analysed. It is seen that the accuracy of the solution is strongly dependent on the number of finite elements used in the calculation. This can be partly attributed to the simplified assumptions used in deriving the geometric stiffness matrix.

Table 3

$\sigma_{cr} = K \frac{\pi^2 E}{12(1-\nu^2)} \left(\frac{h}{a}\right)^2$	Mesh	Coefficient K	error %
simply supported plate 	6x6	4.192	4.8
	9x9	4.044	1.1
	14x14	4.016	0.4
clumped plate 	6x6	5.947	12.0
	9x9	5.506	3.7
	14x14	5.374	1.2
	19x19	5.337	0.5

References

1. R. H. GALLAGHER, *Shell elements*, Proc. World Congress on Finite Element Method in Struct. Mech. Bournemouth, England, 1975.
2. M. D. OLSON, T. W. BEARDEN, *A simple flat triangular shell element revisited*, Int. J. Num. Meths. Eng. **14**, 51 - 68, 1979.
3. R. W. CLOUGH, C. P. JOHNSON, *A finite element approximation for the analysis of thin shells*, Inst. Y. Sol. Struct. **4**, 43 - 60, 1968.
4. H. WENNERSTRÖM, *Nonlinear shell analysis performed with flat elements*, Proc. Int. Conf. Finite Elements in Nonlinear Mechanics, Geilo, Norway, August 1977, pp. 285 - 302.
5. J. H. ARGYRIS, P. C. DUNNE, G. A. MALEJANNAKIS, E. SCHELKE, *A simple triangular facet shell element with applications to linear and non-linear equilibrium and elastic stability problems*, Comp. Meths. Appl. Mech. Eng. **10**, 371 - 403 and **11**, 97 - 131, 1977.
6. M. KLEIBER, *A triangular finite element for large deformation elasto-plastic analysis of arbitrary shells*, Bull. Acad. Polon. Sci. Ser. Sci. Techn. **26**, No 2, 61 - 71, 1978.
7. J. H. ARGYRIS, H. BALMER, M. KLEIBER, U. HINDENLANG, *Natural formulation of large inelastic deformations for shells of arbitrary shape-Application of the TRUMP element*, Comp. Meths. Appl. Mech. Eng. **22**, 361 - 389, 1980.
8. G. HERRIGMOE, P. G. BERGAN, *Nonlinear analysis of free-form shells by flat finite elements*, Comp. Meths. Appl. Mech. Eng. **16**, 11 - 35, 1978.
9. M. KLEIBER, H. STOLARSKI, *Numerical analysis of elastic-plastic shells in the range of large static deformations*, (in Polish), Institute of Fundamental Technological Research, Warsaw 1976, Results obtained in the course of research sponsored by the Centrum Techniki Okrętowej, contract EU/B/246/74.
10. M. KLEIBER, A. ZACHARSKI, *SHELIN — linear finite element analysis of thin free-form shells*, (in Polish), Institute of Fundamental Technological Research, Report No 51/1978, Warsaw.
11. A. ZACHARSKI, *Nonlinear static analysis of thin shells of arbitrary shape*, (in Polish), Ph. D. thesis, Institute of Fundamental Technological Research, Report No 15/1982, Warsaw.
12. P. PERZYNA, *The constitutive equations for rate sensitive plastic materials*, Quart. Appl. Math., **20**, 321 - 332, 1963.

13. O. C. ZIENKIEWICZ, I. C. CORMEAU, *Visco-plasticity and creep in elastic shells—a unified numerical solution approach*, Int. J. Num. Meths. Eng. **8**, 821 - 845, 1974.
14. S. NAGARAJAN, E. P. POPOV, *Plastic and viscoplastic analysis of axisymmetric shells*, Int. J. Sol. Struct. **11**, 1 - 19, 1975.
15. B. KRÅKELAND, *Large displacement analysis of shells considering elasto-plastic and elasto-viscoplastic materials*, Report No 77 - 6, Dec. 1977, Div. of Struct. Mech., The Univ. of Trondheim, Norway.
16. M. KLEIBER, *Natural finite elements and large deformation elasto-viscoplasticity*, Bull. Acad. Polon. Sci. Ser. Sxci. Techn. **26**, 73 - 81, 1978.
17. J. H. ARGYRIS, J. ST. DOLTSINIS, M. KLEIBER, *Incremental discretized formulation in non-linear mechanics and finite strain elasto-plasticity-natural approach Part. II*, Comp. Meths. Mech. Eng. **14**, No 2, 259 - 294, 1978.
18. R. W. CLOUGH, C. A. FELIPPA, *A refined quadrilateral element for analysis of plate bending*, Proc. Conf. Matrix Methods in Struct. Mech., Wright—Patterson, Ohio, 1968.
19. R. BARES, *Tables for the analysis of plates, slabs and diaphragms based on the elastic theory*, 2nd ed., Bauverlay, GmbH., Wiesbaden, 1971, German-English edition.
20. W. KANOK-NUKULCHAI, R. L. TAYLOR, T. I. HUGHES, *A large deformation formulation for shell analysis by the finite element method*, Comp. Struct., Vol. 13, 1981.
21. K. J. BATHER, S. BOLOURCHI, *A geometric and material nonlinear plate and shell element*, Comp. Struct., Vol. 11, 1980.
22. H. PARISH, *Large displacements of shells including material nonlinearities*, Comp. Meth. Appl. Mech. Engng., Vol. 27, 1981.
23. G. DHATT, *Instability of thin shells by the finite element method*, Symp. of Int. Assoc. of Shell Struct., Vienna, 1970.
24. C. TAHIANI, L. LACHANCE, *Linear and non-linear analysis of thin shallow shells by mixed finite elements*, Comp. Struct., Vol. 5, 1975.
25. P. BERGAN, *Nonlinear analysis of plates considering geometric and material effects*, Div. of Struct. Mech. the Norwegian Inst. of Techn., Report No 72 - 1, May 1972.
26. P. BERGAN, G. HORRIGMOE, B. KRÅKELAND, T. SPREIDE, *Solution techniques for non-linear finite element problems*, Int. J. Num. Meth. Engng., Vol. 12, 1978.

Резюме

ЭФФЕКТИВНЫЙ НЕЛИНЕЙНЫЙ АНАЛИЗ ТОНКИХ ОБОЛОЧЕК ПРОИЗВОЛЬНОЙ ФОРМЫ

В работе обсуждены основные аспекты статического нелинейного анализа оболочек произвольной формы методом конечных элементов. Применено относительно простые конечные элементы облегчая таким образом введение данных и интерпретацию полученных результатов. Учтены проблемы больших перемещений оболочек и неупругих свойств материала. Обсуждены также вопросы анализа линеаризированной устойчивости оболочек. Работа иллюстрирована численными примерами.

Streszczenie

W pracy przedstawiono podstawy statycznej, nieliniowej analizy powłok dowolnego kształtu metodą elementów skończonych. Zastosowano względnie proste elementy skończone, upraszczając w ten sposób wprowadzanie danych wejściowych oraz interpretację otrzymywanych wyników. Uwzględniono problematykę dużych przemieszczeń powłok oraz niesprężyste własności materiału. Omówiono również zagadnienie analizy zlinearyzowanej stateczności powłok. Praca zilustrowana jest licznymi przykładami.